Twelfth Australasian Fluid Mechanics Conference
The University of Sydney, Australia 1995

NUMERICAL SIMULATION OF FLOW DUE TO IMPACTING DROPS

D.E. Morton[1], M.J. Rudman[2], J.-L. Liow[1]

[1] G.K. Williams Cooperative Research Centre for Extractive Metallurgy
Department of Chemical Engineering
The University of Melbourne
Parkville, Victoria
Australia

[2] Commonwealth Scientific and Industrial Research Organisation (CSIRO)
Division of Building, Construction and Engineering
Highett, Victoria
Australia

ABSTRACT

In this paper a computer code is introduced that allows the splash resulting from the impact of liquid drops onto flat liquid surfaces to be simulated. The cavity shapes, cavity depths and resulting secondary jets predicted by the simulations are used to quantitatively compare the numerical results to experimental images obtained from high speed movies for two different sets of drop impact parameters. This study is the first time such a detailed comparison has been made and provides an excellent assessment of the simulations. Although cavity shapes and depths are in good agreement with experiment, the secondary jets formed from the collapse of the impact cavity are less well predicted. The reasons for these discrepancies are discussed and the steps currently being undertaken to rectify the situation are described.

INTRODUCTION

The events following the impact of liquid drops onto liquid pools has fascinated researchers for more than a century. The photographs of Worthington (1882) first revealed the complexity of the fluid flow resulting from drop impacts on deep pools. Impact caused the formation of a cavity, which is hemispherical at maximum depth, before collapsing to form a vertical jet which subsequently became known as the Rayleigh jet. Worthington reported that, depending on the height from which drops were released, the Rayleigh jet became unstable with break-up producing droplets. Other researchers have since identified the natural and industrial significance of splashing. The impact of raindrops on puddles enhances soil erosion (Ferria and Singer, 1985) and produces droplets which have been identified as carriers of bacteria and spores (Fitt and Shaw, 1989). Splashing is a problem during the application of industrial coatings since it results in an uneven surface. Apart from the obvious safety hazards, splashing of molten metals during ingot pouring produces imperfections which affect subsequent downstream processing.

Extreme deformation of free surfaces and the influence of surface tension makes simulation of flow resulting from a drop impact a challenging computational fluid dynamics (CFD) problem. Previous attempts at numerical simulation of splashing have failed to provide an understanding of the mechanisms of splash formation. The simulations of Harlow and Shannon (1967) were not in agreement with experimental observation due to insufficient spatial resolution and a failure to include surface tension effects. Other numerical studies (Ogũz & Properetti, 1990 and Trapaga & Szekely, 1991) have included surface tension but the reliability of results is difficult to assess since no detailed comparison with experimental observation was reported. In this paper, the results of a computer code (GKMAC) are quantitatively compared with experimental images of splashing liquid drops taken from high speed movies.

NUMERICAL METHOD

The incompressible, isothermal Navier-Stokes equations are written in non-dimensional form as

$$\nabla \cdot \mathbf{U} = 0 \quad (1)$$

$$\frac{\partial \mathbf{U}}{\partial t} + \nabla \cdot (\mathbf{UU}) = -\nabla P + \frac{1}{Re}\nabla \cdot \tau + \frac{1}{We}\mathbf{S} + \frac{1}{Fr}\hat{\mathbf{g}} \quad (2)$$

where $\mathbf{U}$ is the velocity field, P is pressure, τ is the viscous stress tensor, $\mathbf{S}$ is the non-dimensionlised surface tension force, $\hat{\mathbf{g}}$ is the normalised gravity vector, Re is the Reynolds number (based on the drop diameter D and impact velocity U_0), We is the Weber number ($We = \rho {U_0}^2 D/\sigma$) and Fr is the Froude number ($Fr = {U_0}^2/gD$).

GKMAC solves eqns. (1) and (2) using a finite difference method based on the MAC method (Welch et. al, 1965). The domain is discretised using a uniform

mesh of rectangular cells. Velocities are evaluated at cell faces and pressure is evaluated at cell centres. The solution algorithm employed by GKMAC has previously been reported elsewhere (Morton et al., 1995). Discussion of GKMAC is limited to the underlying algorithm and new features implemented in the code.

Momentum and pressure fields are solved using a two-step projection method. At the beginning of each time step a first estimate of the new velocity field ($\mathbf{u}^*$) is estimated from a finite difference approximation of eqn. (2) with the pressure field evaluated at the previous time step. A Poisson equation for a pressure correction (δp) is solved to project $\mathbf{u}^*$ onto a divergence-free velocity field:

$$\nabla^2(\delta p) = \nabla \cdot \mathbf{u}^* \tag{3}$$

Equation (3) is solved iteratively using a multi-grid approach. The effectiveness of the multi-grid solver is considerable, with simulations of impacting drops at a resolution of 256×256 requiring an average amount of work equivalent to 40 fine grid iterations – standard SOR had generally failed to converge after 2000 iterations.

To the best of the authors' knowledge, GKMAC represents the first implementation of a multi-grid method to solve for fluid flow with free surfaces. The successful implementation of the mult-grid algorithm relies on assigning full, empty and surface cells on coarse levels in addition to the finest level. This allows the application of appropriate boundary conditions at the free surface at all levels, (see Morton et al., 1995 for details).

Free surface tracking is achieved by solving an equation for a scalar 'colour' or 'Volume-of-Fluid' (VOF) function C.

$$\frac{\partial C}{\partial t} + (\nabla \cdot \mathbf{U}C) = 0 \tag{4}$$

The colour function takes a value of 1.0 in cells filled with fluid, a value of 0.0 in cells devoid of fluid and intermediate values in cells through which the interface passes. To maintain sharp interfaces, a finite difference solution of eqn. (4) must result in minimal numerical diffusion. GKMAC uses a approach based on the flux corrected transport methodology of Zalesak (1979) for VOF advection.

Because surface tension influences the shape and behaviour of the cavity and the Rayleigh jet formed following drop impact, GKMAC includes an implementation of the Continuum Surface Force (CSF) model of Brackbill et al. (1992) in which the surface tension force ($\mathbf{S}$) is approximated by a body force,

$$\mathbf{S} \approx \frac{1}{We}\kappa\nabla\tilde{C}. \tag{5}$$

Here, $\tilde{C}$ is a smoothed color function and the curvature κ is is given by

$$\kappa = \frac{1}{|\,\mathbf{n}\,|}\left[\left(\frac{\mathbf{n}}{|\,\mathbf{n}\,|}\cdot\nabla\right)|\,\mathbf{n}\,| - (\nabla\cdot\mathbf{n})\right] \tag{6}$$

Cell centred normals ($\mathbf{n}$) are evaluated from gradients of a smoothed colour function,

$$\mathbf{n} = \nabla\tilde{C} \tag{7}$$

EXPERIMENTAL PROCEDURE

The experimental apparatus developed to film the events following the impact of water drops is shown in Fig. 1.

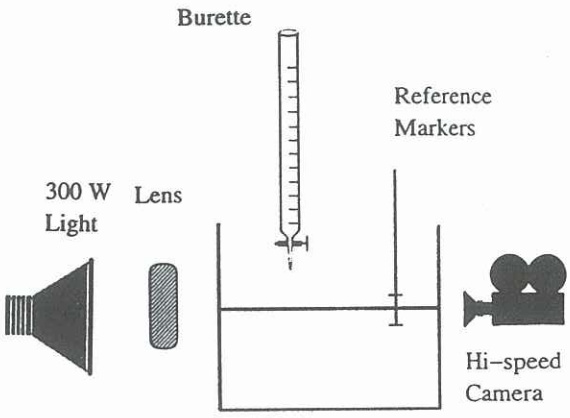

Figure 1: SCHEMATIC OF EXPERIMENTAL APPARATUS

Splash formation was filmed for water drops released from heights of 170mm and 400mm from the surface of a water pool 70mm in depth. For each experimental run the burette valve was adjusted to release drops at a rate of 1.5–2.0 Hz. At these frequencies, the time between each drop was sufficient to ensure that each impact could be regarded as an independent event. The Hycam high speed movie camera was operated at 3000 frames per second. A 300W light source was focussed onto the splash area using a Fresnel lens with a sheet of tracing paper covering the front surface to reduce glare.

EXPERIMENTAL RESULTS

Figures 2 (a)&(b) are high speed movie images of the jets formed following impact of a water drop from heights of 170mm and 400mm respectively. These heights correspond to impact speeds of 1.83 m/s and 2.80 m/s, Reynolds numbers of 5479 and 8400. Weber numbers of 136 and 322 and Froude numbers of 114 and 266 respectively. Each impact resulted in the formation of a hemispherical cavity, at maximum depth, before collapse resulted in the formation of a vertical Rayleigh jet. In both cases the jet became unstable and broke up to produce droplets.

The notable difference between the two jets (first reported by the authors elsewhere , Cullinan et al., 1993) are the shape at maximum height and the behaviour during break-up. The jet formed due to the low momentum impact ($Fr = 114$) was tapered in shape and broke up to produce multiple drops with diameters less than that of the original impacting drop. For the high momentum impact, ($Fr = 266$) the Rayleigh jet formed was cylindrical in shape with break-up producing two drops with diameters similar to the diameter of the impacting drop.

NUMERICAL RESULTS

Figures 3(a)&(b) are the free surface profiles predicted by GKMAC for a 3 mm drop impacting a deep

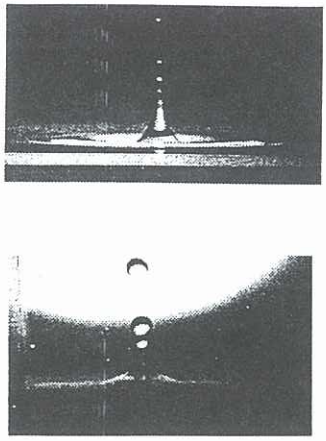

Figure 2: HIGH SPEED MOVIE IMAGES OF SPLASHING DROPS FOR (a) $Fr = 114$, $Re = 5479$, $We = 136$ and (b) $Fr = 266$,$Re = 8440$, $We = 322$. THE TIMES INDICATED ARE NON-DIMENSIONALISED BY THE IMPACT SPEED U_o AND DROP DIAMETER D.

water pool at Froude numbers of 113 and 266 respectively. Simulations were performed on a 256×256 mesh. The flow domain was equivalent to $9D$ in both diameter and height and the liquid pool was 4.5 drop diameters in depth. Simulations were begun at the instant before the drop impacted the pool surface. The drop was initially spherical and travelling vertically at the impact speed. Each simulation was terminated after 2000 time steps which took approximately 12 hours on a SG Crimson workstation.

COMPARISON TO EXPERIMENT

Qualitative comparison

A qualitative comparison between experimental and simulated results is encouraging. Following drop impact, GKMAC predicted the formation of a cavity which was hemispherical in shape at maximum depth. Simulations also predict that the fluid displaced from the cavity forms an annular ring around the edge of the cavity. The ring of fluid reaches a maximum height before maximum cavity depth is attained and begins collapsing whilst the cavity is almost stationary. This prediction is consistent with observations.

The predicted behaviour of the jet, formed following cavity collapse, compares reasonably with experimental results. For the impact from a height of 170mm, the jet predicted by GKMAC was tapered in shape, although it did not reach a height at which break-up to produce drops was observed to occur. Simulation for drop impact from 400mm predicted a jet which was cylindrical in shape at maximum height. This is consistent with the experimental jets for the same impact conditions, although again the jet failed to reach the height observed experimentally. During collapse of the simulated jet, a drop began to form at the jet tip. Although the drop failed to detach from the jet before the simulation was terminated, this result is encouraging because it is similar to the experimental observation that jet break-up occurs after maximum jet height has been achieved.

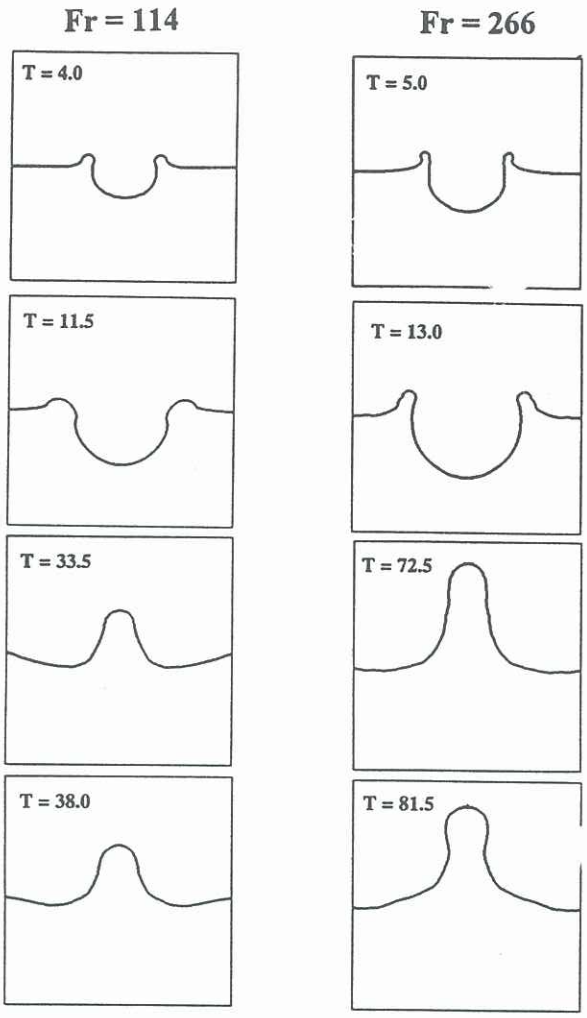

Figure 3: FREE SURFACE PROFILES PREDICTED BY GKMAC FOR (a) Fr=114, Re=5479 and We=136 (b) Fr=266 Re=8400,We=322. THE TIMES INDICATED ARE DIMENSIONLESS

Quantitative comparison

Results of a quantitative comparison of observed and simulated results are presented in tables 1 and 2. The error associated with the experimental measurements is approximately 10% for both maximum cavity depths and times to reach these depths. The predicted cavity depths and time taken to reach these depths are therefore in good agreement with the observed values.

At maximum height, the jets predicted by GKMAC were up to 50% shorter than the observed jets, and consequently the predicted times taken to reach maximum height were significantly less than the times measured from the high speed movie images. Although there is an experimental error of 10% associated with observed jet heights, the comparison of jet heights indicates that GKMAC requires improvement if it is to provide accurate quantitative information about the fluid flow following cavity collapse.

Explanation of discrepancies

Table 1: Comparison of jet and cavity shapes for Fr=114

	Observed	Numerical
Max. cavity depth	2.2D	2.0D
Time to reach max. depth	10.2	11.5
Max. jet height	5.6D	2.8D
Time to reach max. height	44.2	33.4

Table 2: Comparison of jet and cavity shapes for Fr=266

	Observed	Numerical
Max. cavity depth	2.3D	2.0D
Time to reach max. depth	10.8	13.0
Max. jet height	6.3D	4.0D
Time to reach max. height	70.0	54.6

There are several factors that contribute to the discrepancies between observed and predicted jet behaviour. Discretisation error is currently first order in both time and space. This low-order accuracy results in significant numerical diffusion and artificially dissipates momentum transferred to the liquid pool during drop impact and to the Rayleigh jet during cavity collapse. As a result, the potential energy of the cavity at maximum depth will be reduced, as will the height the jet may attain. A higher order scheme for momentum advection is currently under development to reduce the effect of numerical diffusion.

The use of uniform grid spacing and the need for rigid boundaries to be placed a significant distance from the impact site, means that even for a 256 × 256 grid, the jet is poorly resolved. This poor resolution is thought to have two effects. The first is failure to resolve the growth of waves on the jet surface which are responsible for the instability which produces drop detachment. The second is related to the CSF surface tension model which smooths the surface force over a finite fluid volume. A less localised surface will also lead to damping of surface waves and so further hinder the break-up of the jet. A mesh with variable spacing will allow resolution of surface waves and produce a more localised surface force.

CONCLUSIONS

A comparison of simulated results with high speed movie images has shown that the numerical approach adopted in the GKMAC code satisfactorily predicts the fundamental features of the fluid flow resulting from the impact of a liquid drop on a deep liquid pool. Impact of a water drop is followed by the formation of a cavity which is hemispherical at maximum depth. Pool fluid displaced from the cavity appears above the original level of the pool as an annular rim of fluid. The maximum cavity depths and time to reach these depths were within 20% of the observed values indicating that GKMAC provides reliable quantitative information about fluid flow during cavity formation. Jets predicted following cavity collapse were of similar shape compared to the jets observed during experiments, although the jets predicted by simulation were shorter than those observed experimentally. In addition, GKMAC failed to predict jet break-up and drop detachment. These discrepancies have been attributed to the combined effects of numerical diffusion and insufficient resolution of the jet surface. Solutions to these problems are currently being implemented.

ACKNOWLEDGEMENT

Funded by the ARC using facilities provided by the G.K. Williams Cooperative Research Centre for Extractive Metallurgy (a joint venture between the CSIRO Division of Minerals and the Department of Chemical Engineering, The University of Melbourne) and the CSIRO Division of Building, Construction and Engineering.

REFERENCES

Brackbill, J.U., Kothe, D.B. and Zemach, C., 1992, 'A Continuum Method for Modeling Surface Tension', *J. Comput. Phys.*, **100**, 335-354.

Cullinan, V.J., Morton, D.E., Liow., J.-L. and Gray, N.B., 1993, 'Splash Formation from Impinging Liquid Drops', *Proceeding of APPCHE/CHEMECA '93*, Vol. 2 43-48, Melbourne, Australia.

Engel, O.G, 1966, 'Crater Depth in Fluid Impacts', *J. App. Phys.*, **37**, 1798-1808, (1966).

Ferreira, A.G., Singer, M.J., 1985, 'Energy Dissipation for Water Drop Impact into Shallow Pools', *Soil Sci. Soc. AM. J.*, **49**, 1537-1541.

Fitt, B. and Shaw, M., 1989, 'Transports of Blight', *New Scientist*, **August**, 25-27.

Harlow, F.H. and Shannon J.P., 1967, 'The Splash of a Liquid Drop', *J. App. Phys.*, **38**, 10, 3855-3866.

Hirt, C.W. and Nichols, B.D., (1981) 'Volume of Fluid (VOF) Methods for the Dynamics of Free Boundaries', *J. Comput. Phys.* **39** 201-225.

Morton, D.E., Rudman, M.J. and Liow, J.-L., 1995, 'Numerical simulation of splashing phenomena', *Proceeding of 9th International Conference on Numerical Methods in Laminar and Turbulent Flow*, Atlanta, Georgia, USA, 1120-1132.

Ogũz, H. and Prosperetti, A., 1990, 'Bubble Entrainment by the Impact of Drops on Liquid Surface', *J. Fluid Mech.*, **219**, 143-179.

Trapaga, G. and Szekely, J., 1991, 'Mathematical Modeling of the Isothermal Impingement of Liquid Droplets in Spraying Processes', *Metall. Trans. B* , **22B**, 901-914.

Welch, J.E., Harlow, F.H., Shannon, J.P. and Daly, B.J., 1965, 'The MAC Method – A Computing Method for Solving Viscous, Incompressible, Transient Fluid Flow Problems involving Free Surfaces', *Los Alamos Scientific Laboratory Report* **LA–3425**.

Worthington, A.M., 1882, 'On Impact with a Liquid Surface', *Proc. Roy. Soc.*, **25**, 217-230.

Zalesak, S.T., Fully Multidimensional Flux-Corrected Transport Algorithms for Fluids, *J. Comput. Phys.*, **31**, 335–362, (1979).